Structural Study of the Interaction between the SIV Fusion Peptide and Model Membranes†

A. Colotto,‡ I. Martin,§ J.-M. Ruysschaert,§ A. Sen,|| S. W. Hui,|| and R. M. Epand*,‡

Department of Biochemistry, McMaster University, Health Sciences Centre, 1200 Main Street West, Hamilton, Ontario, Canada L8N 3Z5, Laboratoire de Chimie Physique des Macromolecules aux Interfaces, Université Libre de Bruxelles, Campus Plaine CP 206/2, Boulevard du Triomphe 1050, Bruxelles, Belgium, and Biophysics Department, Roswell Park Cancer Institute, Buffalo, New York 14263

Received August 21, 1995; Revised Manuscript Received November 16, 1995⊗

ABSTRACT: It has been shown that there is a correlation between the fusogenecity of synthetic peptides corresponding to the N-terminal segment of wild-type and mutant forms of simian immunodeficiency virus gp32 (SIV) and their mode of insertion into lipid bilayers. Fusogenic activity is only observed when the peptide inserts into the bilayer with an oblique orientation. Since bilayer destabilization is a necessary step in membrane fusion, we investigate how fusion peptides, which insert at different orientations into lipid bilayers, structurally affect model membranes. We use X-ray diffraction to investigate the structural effects of two synthetic peptides on three different lipid systems. One peptide corresponds to the wild-type sequence (SIVwt), which inserts into the membrane at an oblique angle and is fusogenic. The other peptide has a rearranged sequence (SIVmutV), inserts into the membrane along the bilayer normal, and is nonfusogenic. Our results are expressed through different structural effects, which depend on the lipid system: for example, (i) disordering of the L_α phase as evidenced by the broadening of the diffraction peaks, (ii) morphological convertion of multilamellar vesicles into unilamellar vesicles, (iii) decrease of the hexagonal phase cell parameter when SIVwt is added, and (iv) change in the conditions for the formation of cubic phases as well as its kinetic stability over a range of temperatures. Some of these observations are explicable based on the fact that the SIVwt destabilizes bilayers by inducing a negative monolayer curvature, while the SIVmutV destabilizes bilayers by inducing a positive monolayer curvature. Finally, we present a model which describes how these findings correlate with fusogenic activity and fusion inhibitory activity, respectively.

Enveloped viruses infect their host cells by fusing with either the plasma membrane or with the endosomal membrane, after endocytosis of the virion (Ohnishi, 1988; Hoekstra & Wilschut, 1989; Marsh & Helenius, 1989). Fusion activity relies on membrane glycoproteins in the viral envelope which mediate membrane merging (White et al., 1983; Düzgünes, 1985). Studies of synthetic peptides corresponding to the N-terminal domain of the transmembrane glycoprotein showed that at least part of the properties attributed to the glycoprotein depends on a limited stretch of its N-terminal domain (Martin et al., 1991). In fact, synthetic peptides corresponding to the so-called "fusion domain" of the influenza virus hemaglutinin are able to induce fusion of lipid vesicles (Wharton et al., 1988). It has even been shown that a model HIV-I fusion peptide can promote the mixing of aqueous contents of liposomes (Nieva et al., 1994).

There seems to be a correlation between the fusogenicity of synthetic modified peptides corresponding to the N-terminal of simian immunodeficiency virus (SIV)[1] gp32 and their mode of insertion into lipid bilayers (Horth et al., 1991; Epand et al., 1994). It has been proposed that the orientation of the peptide in the lipid bilayer changes as a consequence of the rearrangement of the amino acid sequence which results in a change of the distribution of hydrophobicity around the helix axis, without changing the α-helicity (Brasseur et al., 1990; Horth et al., 1991). Fusogenic activity is only observed when the peptide inserts into the bilayer with an oblique orientation (Horth et al., 1991). It has been suggested that a possible mechanism by which peptides which insert into membranes at an oblique angle perturb bilayer structures is by expanding the center of the bilayer more than the bilayer surface, thus increasing negative curvature strain and destabilizing the bilayer relative to the formation of inverted phases. This would occur as a result of precession of the fusion peptide causing the phospholipids in close contact with the peptide to become tilted with respect to the bilayer normal (Brasseur et al., 1990). The destabilization of the lipid bilayer within the area of adhesion is a crucial step in membrane fusion (Chernomordik et al., 1995). Evidence of viral fusion peptides destabilizing bilayers by inducing a negative curvature strain in the membrane have been presented for the amino terminal of the HA2 protein of influenza virus (Epand & Epand, 1994; Epand et al., 1992) and for the N-terminal of the gp32 glycoprotein of SIV (Epand et al., 1994).

† We acknowledge the financial support obtained from the Medical Research Council of Canada, Grant No. 7654.

‡ McMaster University.
§ Université Libre de Bruxelles.
|| Roswell Park Cancer Institute.

⊗ Abstract published in *Advance ACS Abstracts,* January 1, 1996.

[1] Abbreviations: SIV, simian immunodeficiency virus; SIVwt, wild-type N-terminal of simian immunodeficiency virus gp32; SIVmutV, mutant type N-terminal of simian immunodeficiency virus gp32; *R*, peptide to lipid molar ratio; MLV, multilamellar vesicles; MeDOPE, monomethyldioleoylphosphatidylethanolamine; DPoPE, dipalmitoleoylphosphatidylethanolamine; DOPC, dioleoylphosphatidylcholine; DOPE, dioleoylphosphatidylethanolanine; HFP, hexafluoropropanol; DSC, differential scanning calorimetry; EM, electron microscopy.

0006-2960/96/0435-980$12.00/0

In this work we investigate how the orientation of hydrophobic viral fusion peptides is related to their structural effect on lipid polymorphism and try to correlate this with membrane fusion. We use X-ray diffraction to study the interaction of two different peptides, which resemble the N-terminus of the simian immunodeficiency virus (SIV) glycoprotein gp32, with model membranes. These two peptides have the same amino acid composition, and hence hydrophobicity, but altered amino acid sequences. The two peptides are

SIV wt: GlyValPheValLeuGlyPheLeuGlyPheLeuAla

SIV mutv: GlyValPheGlyValAlaLeuLeuPheLeuGlyPhe

The first peptide corresponds to the wild-type sequence (SIVwt), which inserts into the membrane at an oblique angle to the membrane normal (Martin et al., 1991). The other one has a rearranged sequence (SIVmutV) and inserts into the membrane perpendicular to the plane of the bilayer (Martin et al., 1994). Our results indicate that both peptides have a bilayer destabilizing effect. However, contrary to the SIVwt which destabilizes the bilayer by inducing a negative curvature strain, the SIVmutV peptide destabilizes the bilayer by inducing a positive curvature strain.

The results reported in this work reinforce the idea that the primary role of active viral fusion peptides is to destabilize bilayers by increasing negative curvature strain (Epand et al., 1994). We propose a model to illustrate how the two opposite bilayer destabilizing effects correlate with a fusogenic action and expected fusion inhibitor action of the two peptides, respectively. The anticipated inhibitory action of the SIVmutV is based on analogy with lysolecithins which also inhibit fusion (Chernomordik et al., 1993; Yeagle et al., 1994) and are known to be a type I structures promoter. Type I structures are those with phospholipid headgroups facing toward the outside of the structure such as occurs in micelles. In type II structures, phospholipids have the opposite orientation such as with inverted micelles or with the inverted hexagonal phase (H_{II}). We have also demonstrated that one of the actions of the lysophosphatidylcholine is to prevent the oblique insertion of the SIV fusion peptide into the membrane (Martin et al., 1993; Martin & Ruysschaert, 1995).

MATERIALS AND METHODS

Sample Preparation. The lipids, monomethyldioleoylphosphatidylethanolamine (MeDOPE; lot no. 181mpe-53), dipalmitoleoylphosphatidylethanolamine (DPoPE; lot no. 161pe-16), dioleoylphosphatidylcholine (DOPC; lot no. 181pc-115), and dioleoylphosphatidylethanolanine (DOPE; lot no. 181pe-159), were purchased from Avanti Polar Lipids (Alabaster, AL). Lipids were used without further purification. 1,1,1,3,3,3-Hexafluoro-2-propanol (HFP; lot no. 64H3493), pure, was purchased from Sigma (St. Louis, MO) and used as solvent for the preparation of lipid films to make multilamellar vesicles (MLVs).

Lipid films were prepared by adding ice-cold HFP to a weighed amount of lipids, vortexing the mixture until a homogeneous solution could be achieved, and evaporating the HFP under a stream of N_2. In order to remove residual traces of HFP, samples were placed under vacuum for 2 h and then lyophilized overnight. The films were subsequently hydrated by adding ca. 2 mL of 20 mM Hepes, 150 mM NaCl, and 1 mM EDTA, pH 7.4, buffer and were vortexed at room temperature. Differential scanning calorimetry (DSC) and X-ray diffraction experiments have shown that samples prepared in this way still contained residues of HFP, which caused a dramatic decrease in the lamellar to hexagonal phase transition temperature and highly disordered the L_α phase (data not shown). Therefore, the samples were centrifuged after hydration in order to separate the lipid phase from the aqueous phase. The aqueous phase was removed and replaced with fresh buffer, and the sample was vortexed again. This procedure was repeated three times. DSC and X-ray data of the samples prepared in this way gave no evidence of the presence of HFP residues. Samples containing peptide were prepared in the same way as described above. Weighed amounts of peptide in HFP were added to weighed amounts of lipids in HFP so as to give the desired peptide to lipid molar ratios.

X-ray Diffraction Experiments. Nickel-filtered Cu Kα ($\lambda = 1.54$ Å) X-ray was obtained from a Rigaku-Denki (Model RU-200B) rotating anode. X-rays were focused using a Frank's type camera and recorded using a position-sensitive proportional counter TEC Model 205 (Sen et al., 1990). Unoriented lipid dispersions, prepared as described above, were measured in 1.5 mm Ø glass capillaries in all diffraction experiments. The specimen temperature (±0.5 °C) during X-ray diffraction was controlled by a thermoelectric device. For the measurement of lattice spacing vs temperature, the typical protocol involved stepwise heating the specimen in intervals of 10 °C in the temperature range of the L_α phase, in intervals of 1−2 °C in the proximity of the bilayer to hexagonal phase transition temperature (T_H), and then in intervals of 10 °C above T_H. The systems were allowed to equilibrate for about 5 min at the desired temperature before measurement. The X-ray exposure times were typically of 5−15 min using the position-sensitive detector. Figures 1, 3, 7, 10, and 12 present such results. It should be noted that these diffractograms must be symmetrical for the nonoriented samples we are using. Deviations from a symmetrical pattern are largely due to position-dependent variations in detector efficiency. The center of all of the diffractograms have two large positive peaks on either side of a deep trough. This pattern is a normal consequence of the presence of the beam stop and is not a result of diffraction by the sample. Because of the small size of the figures, some of the higher, weaker orders cannot easily be seen in the figure but are readily observed in the original data and are referred to in the text. Figure 5 is derived from an exposure on Kodak (Rochester, NY) DEF 5 Scientific Imaging Film.

The spacing of the peaks in the diffractograms allows us to specify the nature of the packing symmetry of the phase, i.e., L, Q, or H, while the distance of peaks from the center of the symmetrical powder pattern allows us to calculate the repeat or *d*-spacing of that phase. This is done, after baseline subtraction, for all of the easily resolvable orders and the calculated d-spacing is given as an average of these values.

Typical absolute lattice spacing, calibrated against C19 ($d = 26.2$ Å), is accurate to ±0.5 Å for lattices up to ∼80 Å and to ±1−2 Å for larger lattices.

Freeze−Fracture Electron Microscopy. Samples were frozen by the rapid-freeze sandwich method as described previously (Hui et al., 1985). Briefly, 0.1 μL of the lipid dispersion was sandwiched between two thin copper plates and quickly plunged in liquid propane, without any cryoprotectant. The frozen samples were fractured at −120 °C

in a modified Polaron E7500 unit. Replicas of the fracture surfaces were prepared by evaporating platinum followed by carbon. The replicas were washed with a 1:1 chloroform−methanol mixture and examined in a Hitachi H-600 electron microscope.

RESULTS AND DISCUSSION

The effects of the two SIV peptides, the wild-type and the mutant form, on three different lipid systems were investigated. The results are reported below.

MeDOPE. Dispersions of MeDOPE in aqueous solutions are found to form different ordered structures depending on both the temperature and thermal history of the sample. The polymorphic behavior of this lipid has been extensively studied with a large variety of techniques (Gruner et al., 1988; Siegel & Banschbach, 1990; Gagne et al., 1985; Silvius & Brown, 1986; Van Gorkom et al., 1992). Basically, this system may order in three different structures: lamellar, cubic (Pn3 or Pn3m), and hexagonal. The cubic structures are observed, or not, as stable or metastable phases between the lamellar and hexagonal phases. This depends on the time scale of the temperature scan across the lamellar to hexagonal phase transition (Van Gorkom et al., 1992). If the sample is heated relatively fast (40 °C/h), the system will undergo a phase transition from the liquid crystalline lamellar phase (L_α) to a type II hexagonal phase (H_{II}) at $T_H = 60-66$ °C (depending on the sample concentration). If the system is heated relatively slowly (<13 °C/h), it will undergo a phase transition from the lamellar to a cubic phase at a temperature, lower than T_H, which will depend on scan rate and sample history. It has also been reported that the thermotropic phase behavior of this system, as well as its structural dimensions, is highly concentration dependent (Gruner et al., 1988). In the experiments reported below, the samples have been handled such as to have the pure MeDOPE transiting directly from the lamellar to the hexagonal phase. For our samples this occurred at $T_H \sim 60$ °C. The samples were treated in a systematic way in order to ensure reproducibility and for the sake of comparison. Samples were heated in intervals of 10 °C in the temperature range of the L_α phase, in intervals of 1−2 °C in the proximity of T_H, and in intervals of 10 °C again above T_H. The systems were allowed to equilibrate for about 5 min at a desired temperature before measurement. Measurements took from 10 to 15 min. Using this protocol, no traces of cubic phase formation were detectable from the X-ray diffraction measurements for the pure lipid system.

The typical diffraction data obtained for the pure system is shown in Figure 1. Under the experimental conditions used, only the first four order reflections of the lamellar phase (*d*-spacing ratio 1:2:3:4:...) were observed (Figure 1A, the third and fourth orders are clearly seen in the original data). The system transits to the hexagonal phase in what we refer to as an "ordered way". By this we mean that, in the temperature range where the phase transition takes place, lamellar phase domains coexist with hexagonal phase domains. Due to phase coexistence, diffraction peaks from both phases are observed around the phase transition temperature (Figure 1B). Figure 1C shows a typical diffractogram obtained for the H_{II} phase. Five diffraction peaks are observed (*d*-spacing ratios $1:\sqrt{3}:\sqrt{4}:\sqrt{7}:\sqrt{9}$:...). As the temperature is increased, the reflections shift to higher angles, indicating that the hexagonal phase cell parameter decreases (Figure 2). This is a typical result for H_{II} phases and is due

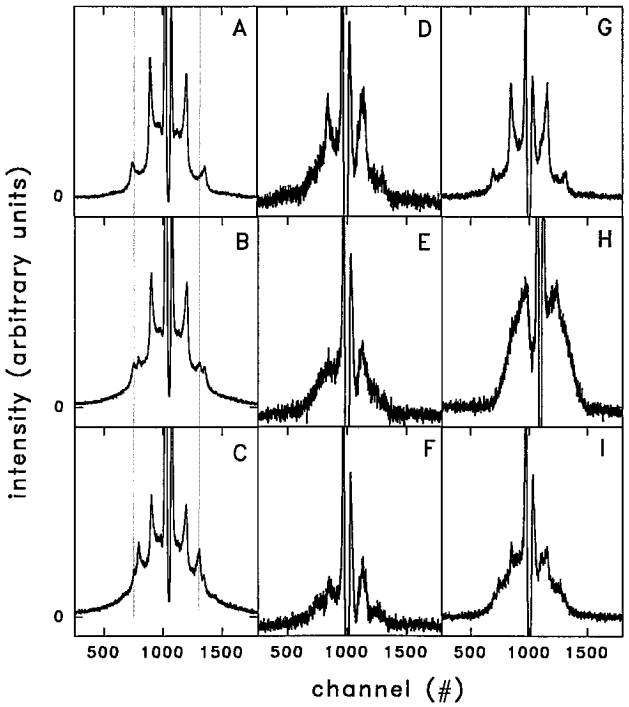

FIGURE 1: X-ray diffraction patterns obtained for the MeDOPE system alone and in the presence of the two peptides studied: MeDOPE (A) at 30 °C, (B) at 60 °C, and (C) at 70 °C; MeDOPE/SIVmutV, $R = 10^{-2}$ (D) at 30 °C, (E) at 60 °C, and (F) at 70 °C; and MeDOPE/SIVwt, $R = 10^{-2}$ (G) at 30 °C, (H) at 60 °C, and (I) at 70 °C.

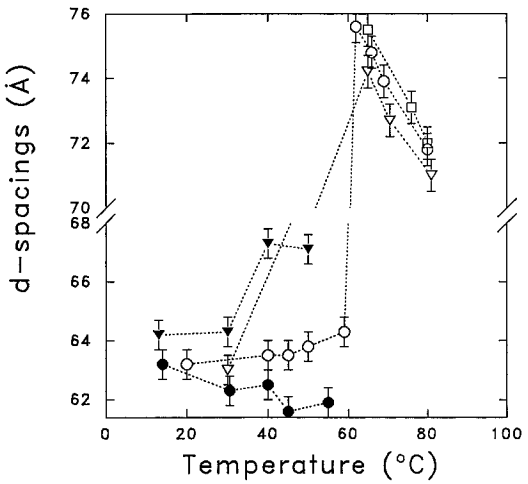

FIGURE 2: *d*-Spacing calculated from the X-ray diffractograms obtained from the system MeDOPE in the presence of the two forms of the SIV fusion peptide studied, at different molar ratios and temperature, respectively: (○) MeDOPE; (▽) MeDOPE/SIVwt, $R = 10^{-2}$; (□) MeDOPE/SIVwt, $R = 5 \times 10^{-2}$; (●) MeDOPE/SIVmutV, $R = 3.3 \times 10^{-3}$; (▼) MeDOPE/SIVmutV, $R = 10^{-2}$. The *d*-spacings were calculated using the Bragg law: $2d \sin \theta = n\lambda$.

to increased curvature strength resulting from acyl chain splay at higher temperatures. With increasing temperature, the bilayer gets thinner and the ratio between the minimal surface and the parallel surface of the polar/nonpolar interface corresponds to an increased molecular wedge shape. Our X-ray diffraction results for the pure system in the lamellar and hexagonal phases, respectively, are in agreement with data previously published (Gruner et al., 1988). However, no phase coexistence in the transition temperature range has been previously shown by X-ray diffraction, to our knowledge, for this system. The coexistence of lamellar and

hexagonal domains is in agreement with a mechanism of transition in which a flattened or ribbon-like tubule structure is formed by zipping the adjacent bilayers along attachment lines, as proposed by Hui et al. (1983), that is, without cubic intermediates. It should be noted that the line attachments must be regularly distributed, or else the ordering of the cylinders in an hexagonal lattice must occur very fast, otherwise no ordered phase would be observed.

The hexagonal phase cell spacing decreases slightly in the presence of the SIVwt (Figure 2). However, the temperature dependence of the cell parameter in the H_{II} phase is the same for both the pure lipid and the peptide-containing system. It should be noted that although the decrease induced in the hexagonal phase *d*-spacing by the peptide is relatively small, it is significant when compared to that induced by dodecane for both MeDOPE and PE/PC mixtures (Gruner et al., 1988). Dodecane, when added to these lipid systems, causes a dramatic decrease in the lamellar to the hexagonal phase transition temperature. This may be a consequence of dodecane relieving the hexagonal phase hydrocarbon packing constraints, rather than by changing the intrinsic radius of curvature of the monolayer. In the case of the SIVwt peptide, for which we have observed a slight decrease in the hexagonal cell parameter, the bilayer-destabilizing effect is likely due to a change in the monolayer intrinsic radius of curvature (the peptide is not likely to be sufficiently hydrophobic to fill the hydrocarbon packing voids among the H_{II} phase cylinders). Smaller cell parameters in the H_{II} phase correspond to a higher negative curvature of the lipid monolayers, unfavorable for bilayer structures. This is in agreement with the idea of the peptide affecting the system due to its oblique orientation in the membrane.

A general result is a decrease in the degree of order of the structures. This disordering effect depends on the peptide content in a directly proportional way, as well as on temperature. The diffraction peaks broaden, indicating a gradual loss of order in both the lamellar and hexagonal phases (Figure 1, panels G and I, respectively). Within the temperature region of the lamellar phase, there is also a decreased order with increasing temperature. At relatively high peptide to lipid molar ratios (e.g., $R = 5 \times 10^{-2}$), the system is completely disordered over the entire range of temperatures studied. No diffraction peaks are observed in either the L_α or the H_{II} phases. There is only a continuous scattering curve, indicative of a highly disordered specimen (like the pattern shown in Figure 1H). It is possible, though, to restore the hexagonal lattice to the system by rapidly increasing the temperature to 70 °C. As shown in Figure 3B, the diffractogram obtained from the peptide containing sample submitted to such a thermal treatment is typical of the hexagonal phase. The diffractogram obtained from the pure lipid system submitted to the same thermal treatment is also shown for comparison and is also characteristic of the H_{II} phase (Figure 3A).

In order to investigate the nature of the disordering effect observed in the diffractograms, lipid/peptide samples were rapidly freeze-quenched from temperatures below and above T_H, respectively, and examined by freeze−fracture electron microscopy. The freeze−fracture micrographs shown in Figure 4 illustrate the morphologies of the pure MeDOPE dispersion at room temperature and of a peptide-containing sample with molar ratio $R = 5 \times 10^{-2}$ both at room temperature and at 60 °C. The micrograph of the pure lipid at room temperature (Figure 4A) shows a typical multilamellar vesicle, with many layers, characteristic of this specimen. Relatively few unilamellar vesicles can be found (not seen in field shown in Figure 4A). Samples with intermediate SIVwt/lipid molar ratios ($R \leq 10^{-2}$; L_α and H_{II} diffraction patterns still seen) contain both MLVs and unilamellar vesicles at room temperature (data not shown). Figure 4B−D show the micrographs from the peptide containing system at 60 °C. The sample was heated in one single fast step to this temperature. This corresponds to the procedure by which we were able to restore the hexagonal ordering of the lipids from a highly disordered condition. The three different coexisting morphologies are as follows: (i) amorphous, Figure 4B; (ii) multilamellar, Figure 4C; and (iii) hexagonal, Figure 4D. In this case, the multilamellar phase does not seem to constitute vesicles, but rather simply stacked lamellae. We propose, on the basis of these results, that the disordering effect we observe in the X-ray diffraction patterns upon addition of peptide is due to gradual vesiculation of neighboring lamellae within the MLVs, which starts as a positional disorder (Guinier, 1963) due to attachments between adjacent bilayers. Part of the broadening of the reflection peaks might also be due to the fact that, upon vesiculation, the size of the MLVs decreases. The transformation of MLVs to smaller vesicles with fewer lamellae may be thermodynamically favorable (Hartung et al., 1994), but the SIVwt peptide may greatly accelerate the rate of this transformation. Once unilamellar vesicles are formed, these structures cannot transit into hexagonal phase rods, and therefore not even a disordered hexagonal phase is formed. However, as has been shown, it is possible to cause these unilamellar vesicles to fuse into MLVs again by submitting them to rapid heating. We suggest that the amorphous

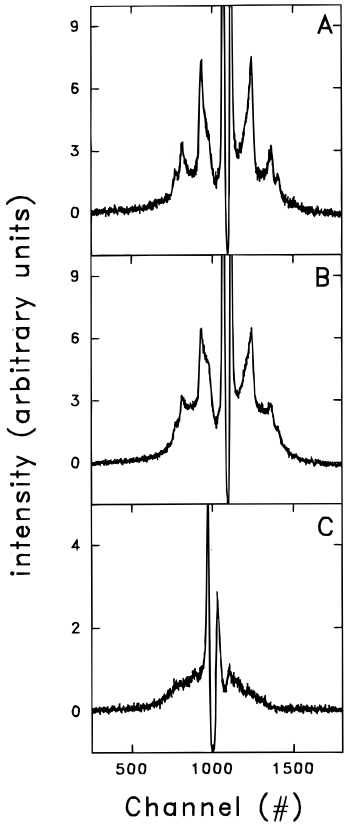

FIGURE 3: X-ray diffraction profiles from MeDOPE samples with and without peptide at 70 °C. Samples were heated in one single fast step starting from room temperature. (A) MeDOPE; (B) MeDOPE/SIVwt, $R = 5 \times 10^{-2}$; and (C) MeDOPE/SIVmutV, $R = 5 \times 10^{-2}$.

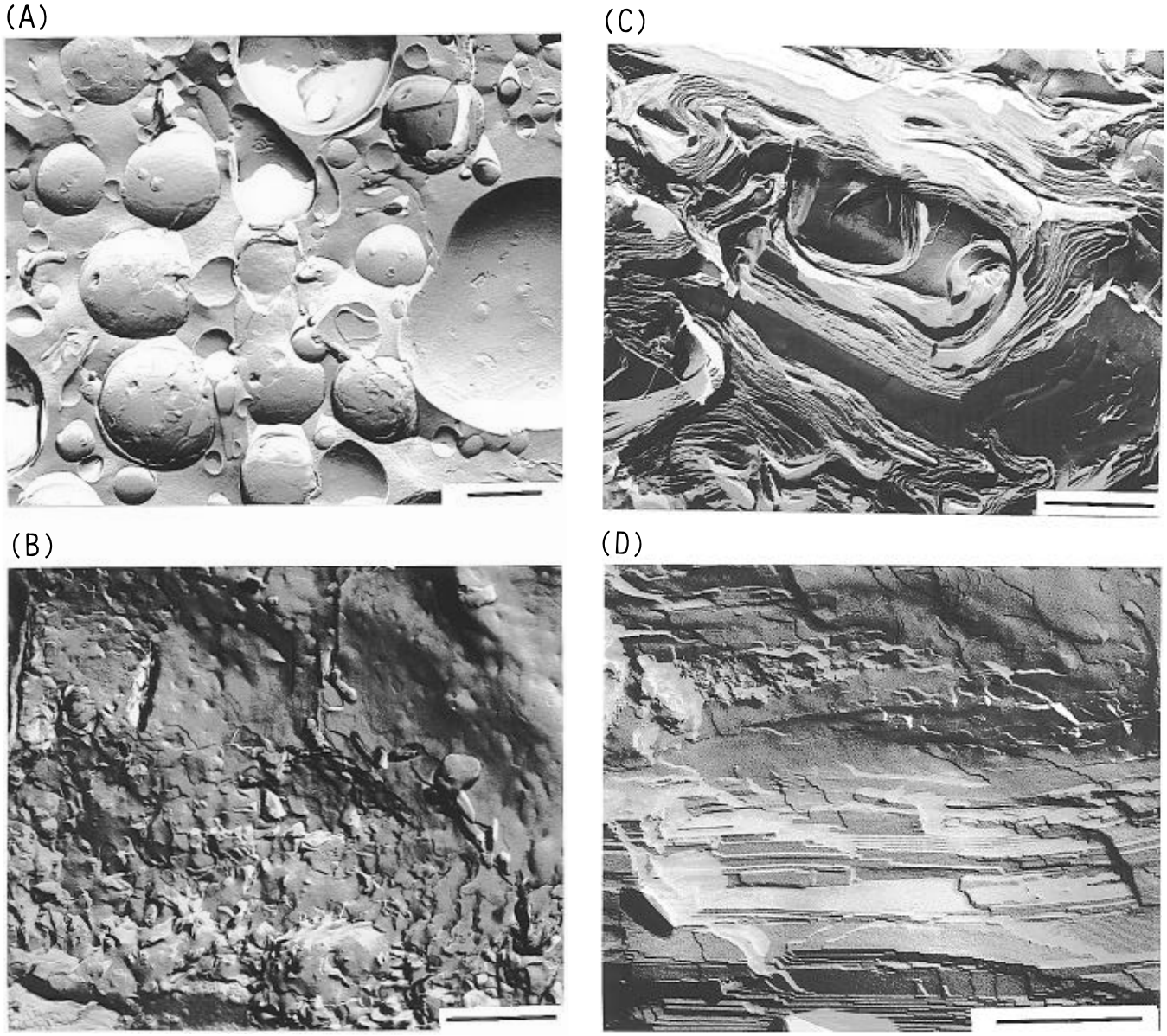

FIGURE 4: Freeze−fracture electron micrographs of (A) MeDOPE at room temperature and (B−D) MeDOPE/SIVwt, $R = 5 \times 10^{-2}$, after being heated to 60 °C. Scale bars represent 50 nm.

morphology observed (Figure 4B) is an intermediate between the unilamellar and multilamellar vesicle structures. It should be noted that the mechanisms proposed for formation of the hexagonal phase imply interlamellar connections between adjacent bilayers in stacked lamellae (Hui et al., 1983).

The SIVmutV peptide also causes a decrease in the degree of order of the MeDOPE system, both when in the lamellar and hexagonal phases (Figure 1D−F). The disordering effect increases with increasing peptide content. At $R = 10^{-2}$, though, differently from the system containing SIVwt, the hexagonal phase is found to coexist with domains of cubic structure for 60 °C $\leq T \leq$ 80 °C (Figure 5). The crystallographic data corresponding to the diffraction picture shown in Figure 5 are listed in Table 1. The hexagonal cell parameter was calculated as the average from the values obtained from the three reflections assigned to this phase and has a value between that obtained for the pure lipid system (75.6 ± 0.5 Å) and that obtained for the SIVwt containing system (72.6 ± 0.5 Å) at the same temperature. The cell parameter obtained for the cubic lattice was calculated as the average from the values calculated from the seven orders of diffraction observed. These reflections were spaced in the ratio of $\sqrt{2}$:$\sqrt{3}$:$\sqrt{6}$:$\sqrt{8}$ $\sqrt{9}$:$\sqrt{11}$:$\sqrt{12}$. The smallest unit cell space groups consistent with orders spaced in these ratios are the Pn3m and Pn3 with a 140 Å cell parameter. Gruner et al. (1988) observed the same lattice for the pure lipid system. In their work, they were able to distinguish nine diffraction orders, including the fourth one. Since the fourth order peak occurs very closely to the sixth one, it is possible that it is not well resolved in our case due to the broadness of the reflections. The value obtained for the unit cell of the cubic lattice of the pure lipid system is slightly lower than the one we obtained (see Table 1). It is essential to note that the cubic phase observed by Gruner's group was formed under completely different conditions than the one induced by the SIVmutV. The cubic phase observed in the pure lipid system formed either when the specimen was held at temperatures lower, but close to, T_H for very long times or when the sample was cooled down through T_H. Upon cooling down, the evolution of the system into a cubic phase was faster, but still slow compared to the cubic phase formation induced by the SIVmutV peptide. In order to obtain the well resolved X-ray patterns they reported,

Table 1: Assignments and Spacings of Reflexions from the Diffractogram Shown in Figure 5

MeDOPE/SIV$_{mt-v}$					literature (MeDOPE)		literature (MeDOPE)	
	cubic		hexagonal		cubic		hexagonal	
d (Å)$_{measured}$	$h^2 + k^2 + l^2$	d (Å)$_{calc}$	$h^2 + k^2 + hk$	d (Å)$_{calc}$	$h^2 + k^2 + l^2$	d (Å)	$h^2 + k^2 + l^2$	d (Å)
101	2	99			2	96.2		
82	3	81			3	78.5		
64.2			1	63.6	4	68.0	1	64.5
56.5	6	57.2			6	55.5		
48.8	8	49.5			8	48.1		
46.1	9	46.7			9	45.3		
43.0	11	42.2			11	41.0		
40.3	12	40.4			12	39.3		
36.8			3	36.7			3	37.2
32.0			4	31.8			4	32.3
	a_{calc} = 140 Å		d_H = 73.5 Å		a = 136 Å		d_H = 74.5 Å	

[a] From MeDOPE/SIVmutV, $R = 10^{-2}$, at 60 °C.

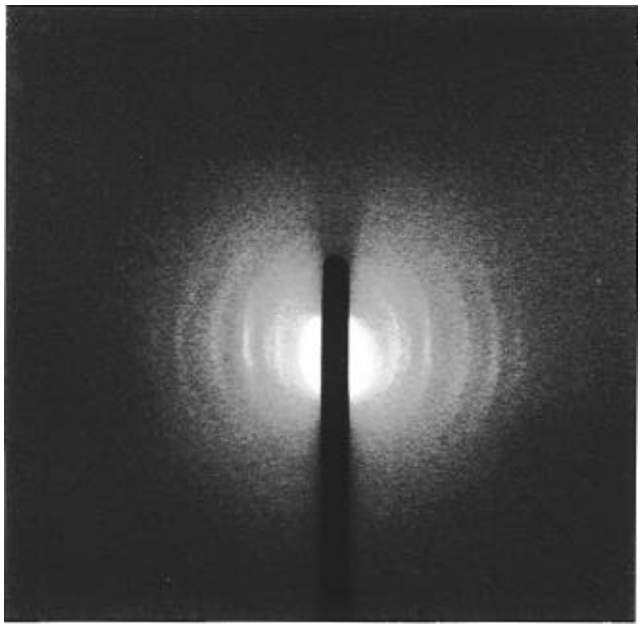

FIGURE 5: X-ray diffractogram taken from the system MeDOPE/SIVmutV, $R = 10^{-2}$, at 60 °C. The corresponding crystallographic data are given in Table 1.

Gruner's group left a sealed X-ray capillary undisturbed for 1.5 years (Gruner et al., 1988)! The observation of cubic structures when the mutant form of the SIV peptide is added to the system is very significant. It indicates that the SIVmutV accelerates the rate of formation of the cubic phase in the system. This effect is opposite to that of alkanes (Van Gorkom et al., 1992) which promote the formation of H_{II} phases. For the hexagonal phase to be stable, the amount of frustration between the monolayer curvature free energy and the free energy of stretching of the lipid chains must be very large (high curvature free energy in the lamellar phase under same conditions). Since cubic phases correspond to a lower amount of frustration (Anderson et al., 1988), the peptide must be lowering the mean curvature energy or raising stretching energy.

Further increase of the peptide to lipid molar ratio up to $R = 5 \times 10^{-2}$, causes a complete disordering of the system. Similar to what has been observed at this molar ratio in the presence of the wild-type peptide in the whole range of temperatures studied (20−80 °C), the typical diffraction patterns from the L_α and H_{II} phases were replaced by a continuous scattering curve. However, in the case of the SIVmutV, we found no thermal treatment which enabled the system to reorder in a hexagonal lattice above T_H (Figure 3C).

Thus the presence of the SIVmutV peptide leads to more facile formation of a cubic phase under conditions where an H_{II} phase is formed with the pure lipid or in the presence of SIVwt. Destabilization of the H_{II} phase by decreasing the curvature energy and the destabilization of the lamellar phase with disordering of the system, at rather low peptide contents, can only be explained by a positive curvature strain caused by the SIVmutV peptide. A positive curvature strain would explain the disordering effect in the L_α phase, because it would cause local bending of the bilayers, analogous to the case of a negative one, resulting in possible contacts between adjacent bilayers. A positive curvature strain would also explain a decrease in the curvature of inverted phases. We propose that the positive curvature contribution of SIVmutV is due to a mismatch between the length of the peptide penetrating the hydrocarbon core and the length of the hydrophobic portion of the bilayer. Such a mismatch would cause a greater expansion of the membrane−solvent interface than of the hydrocarbon region of the bilayer and hence positive curvature.

The effect of the SIVmutV peptide on the L_α cell spacing was not a continuous one. The d-spacing decreased upon addition of peptide up to $R = 3.3 \times 10^{-3}$ and then increased at $R = 10^{-2}$ (Figure 2). Moreover, the temperature dependence of the cell parameter was not the same for the pure lipid and the peptide containing systems. We have no explanation for these observations.

Diffraction patterns of systems taken in the temperature range where the phase transition occurs ($T_H \sim 60$ °C), when any of the peptides were present, consisted of continuous scattering curves, indicative of highly disordered structures. Therefore, we refer to the phase transition in the peptide containing systems as a structurally "disordered" transition. A plausible explanation for this effect might be the creation of irregular attachments between adjacent bilayers due to the local curvature modulation action of the peptides in the monolayers. These irregular attachments create defectuous regions in the stacked membranes, which disturb the kinetics of formation of regular line attachments between neighboring bilayers, thus disordering the evolution of the cylindrical structures from the bilayers. An alternative explanation is that both peptides increase the rate of formation of cubic structures in the system except that in the case of SIVwt the

cubic phase is disordered and/or only transiently stable, while in the case of the SIVmutV it forms a stable structure. Each peptide thus accelerates the rate of formation of the cubic phase in the transition range by destabilizing phases at different sides of the phase transition. It should be noted that both peptides have a bilayer destabilizing effect. However, the results described above indicate that the SIVwt destabilizes the bilayer by inducing a negative curvature (favorable for type II structures), while the SIVmutV destabilizes the bilayer by inducing a positive curvature (favorable for type I structures). This is in agreement with the observed increase of T_H of DPoPE containing SIVmutV (Epand et al., 1994) and also with the nonfusogenicity of the viruses containing the mutant fusion peptide (Martin et al., 1992). Moreover, lysolecithins, which are known to be type I structure promoters, also raise the T_H of various lipid systems (Epand, 1985) and have been shown to have an antifusogenic action (Martin et al., 1994, 1995).

The DOPE/DOPC (3:1) binary system has been suggested to have an intrinsic radius of curvature similar to that of the MeDOPE system (Gruner, 1992). This is supported by the observation that in the temperature range where the two systems are in the hexagonal phase, the d_H versus T curves even overlap. However, the DOPE/DOPC (3:1) transits from the lamellar to the hexagonal phase at $T_H = 47$ °C rather then above 60 °C as with MeDOPE. This indicates that the binary system has a higher intrinsic curvature energy than MeDOPE, but it is not sufficiently different to cause a change in the *d*-spacing of the H_{II} phase. Below the phase transition temperature of MeDOPE, the slope of the *d*-spacing vs temperature curve of the binary system are remarkably different from that of MeDOPE (Gruner et al., 1988). It has been suggested that this behavior, which has been observed with other mixed lipid systems, is due to different ratios of the two lipid species (demixing) in different phases (Tate & Gruner, 1987). A notable aspect is that the DOPE/DOPC (3:1) system has very roughly the same average number of N-linked methyl groups per molecule as does MeDOPE. The diffraction patterns obtained with this lipid mixture (Figure 6A−C), for both the L_α and H_{II} phases, very much resemble those obtained for MeDOPE (Figure 1A−C). Moreover, in the transition temperature range, phase coexistence is observed for this system as well.

As for the MeDOPE system, peptide was added to the binary mixture up to molar ratios $R = 5 \times 10^{-2}$. However, in this case, absolutely no effect on the cell parameter of the hexagonal lattice is observed in the presence of either peptide (Figure 7). It is interesting to note that the addition of dodecane to this same binary system causes a significant increase of the cell spacing at temperatures below the transition temperature of MeDOPE! However, above this temperature, the *d*-spacings are absolutely the same as those obtained for the pure binary system (Gruner et al., 1988). The slope of the L_α repeat spacing versus T, though, is quite peptide dependent. Although a disorder effect is observed in this system too, the system never becomes completely disordered. Even at the highest peptide contents, the L_α and H_{II} diffraction patterns were observed below and above T_H, respectively, for both peptides. Diffractograms obtained for the binary system both in the presence of the wild-type and mutant peptides are shown in Figure 6D−I. The disorder effect is much weaker in this system than in the MeDOPE. This is clearly seen in the temperature range of the phase transition, where diffraction peaks are always observed.

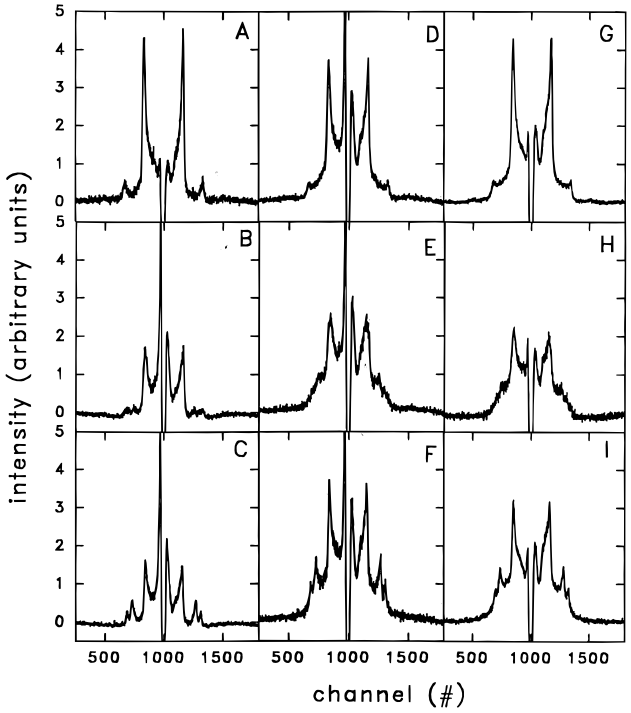

FIGURE 6: X-ray diffraction patterns obtained for the DOPE:DOPC (3:1) mixture alone and in the presence of the two peptides studied: PE:PC (A) at 30 °C, (B) at 47 °C, and (C) at 70 °C; PE/PC/SIVmutV, $R = 5 \times 10^{-2}$ (D) at 30 °C, (E) at 47 °C, and (F) at 70 °C; and PE/PC/SIVwt, $R = 10^{-2}$ (G) at 30 °C, (H) at 47 °C, and (I) at 70 °C.

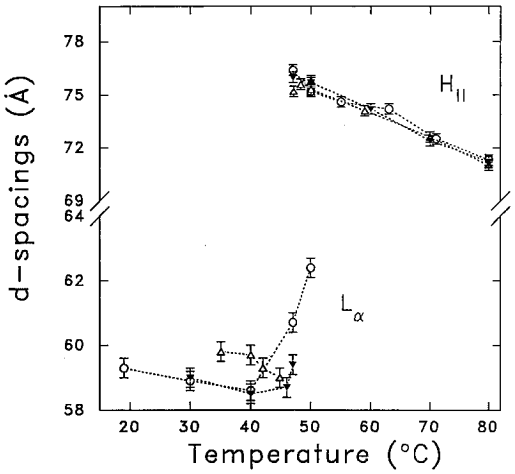

FIGURE 7: *d*-Spacing calculated from the X-ray diffractograms obtained from the lipid mixture DOPE/DOPC (3:1) alone and in the presence of the two forms of SIV fusion peptide studied, respectively: (○) PE/PC; (△) PE/PC/SIVwt, $R = 10^{-2}$; and (▽) PE/PC/SIVmutV, $R = 5 \times 10^{-3}$. The *d*-spacings were calculated using the Bragg law: $2d \sin \theta = n\lambda$.

However, a closer analysis of the first order reflections shows that in this temperature range the peak is much broader, indicating a lower degree of order (Figure 8). The width of the peaks has been calculated by fitting a Gaussian and taking its width at half-height as a measure of the width of the peak. If the broadness of the first order reflections is taken as a measure of the disorder effect induced by the peptides, then the following can be concluded: (i) around T_H the system is more disordered; (ii) the magnitude of the disorder effect is directly proportional to the amount of peptide in the system (Figure 8); (iii) the disorder due to the mutant-V peptide is higher than that due to the wild type (Figure 8). This last point can be rationalized on basis of our results for the

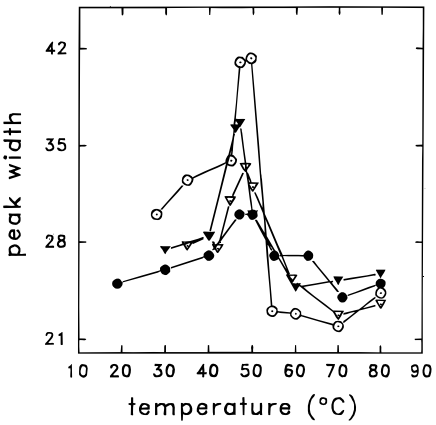

FIGURE 8: Width of the first order peak calculated from the diffraction profiles obtained for the system DOPE/DOPC with and without peptide. Widths were calculated by fitting a Gaussian to the first order peaks measured and taking the width at half-height of the Gaussians as the width of the diffraction peaks. (●) Lipid alone; (▽) PE/PC/SIVwt, $R = 10^{-2}$; (▼) PE/PC/SIVmutV, $R = 5 \times 10^{-3}$; and (⊙) PE/PC/SIVmutV, $R = 3 \times 10^{-2}$.

MeDOPE system. Since the SIVwt is a promoter of type II structures, it will destabilize mainly the L_α phase. The SIVmutV, on the other hand, which is a promotor of type I structures, will destabilize both the L_α and H_{II} phases and therefore cause more disordering in the phase transition region.

The fact that the effects of both peptides on this system are weaker compared to their effects on the MeDOPE system may be explained if the binary system is demixing. This would also allow the peptide to be accommodated in defect regions between lipid domains as well as being excluded from regions of pure DOPC which may be too hydrated or regions of DOPE which would contain a hydrogen-bonded network among headgroups.

DPoPE. In the temperature range investigated in this work (15−80 °C), the DPoPE system presents one phase transition from the L_α to a type II hexagonal phase at $T_H = 43.2$ °C (Epand, 1990). To our knowledge, no diffraction data on this system have been reported thus far. Figure 9A−C shows characteristic diffraction curves obtained for the L_α and hexagonal phases, as well as the curve obtained at about T_H, where phase coexistence is observed. Both the relatively low T_H and the hexagonal phase d-spacing of this system (Figure 10) indicate that this system has a higher intrinsic curvature energy than the other two systems studied in this work. Another remarkable difference between this lipid system and the two former ones lies in the fact that the lipids being PE have stronger hydrogen bonding among the lipid polar headgroups, and the system is less hydrated (Rand et al., 1988). This is also indicated by the lamellar repeat distance (Figure 10).

Addition of either peptide to this system, up to molar ratios $R = 10^{-2}$, did not affect the system in any way, neither by changing the lattice cell parameters of the lamellar or hexagonal phases (Figure 10) nor by introducing disorder into the system. Only at relatively higher peptide to lipid molar ratios, for which the other two lipid systems studied were significantly affected, does the presence of the peptide lead to structural changes. Figure 11 shows the diffractograms obtained for this system in the presence of SIVwt at $R = 5 \times 10^{-2}$. Below T_H, the typical L_α diffraction pattern has been replaced by a set of very low angle reflections superimposed to a continuous scattering curve. The low

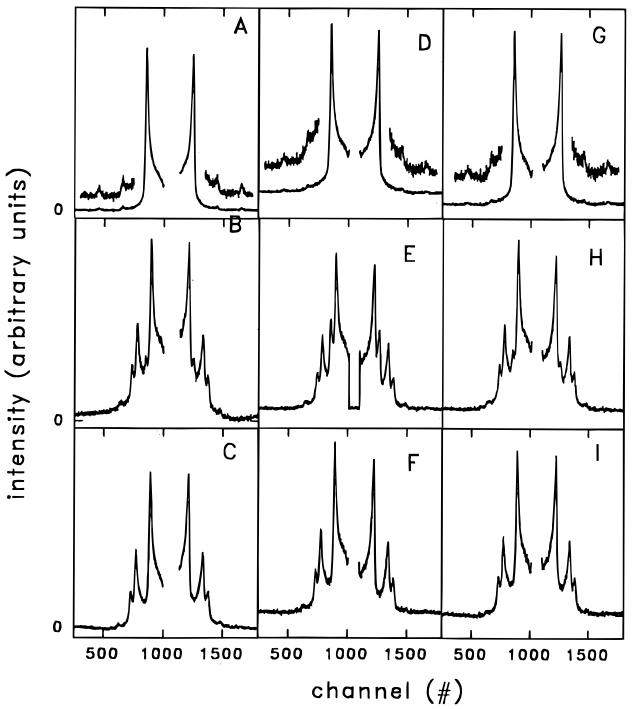

FIGURE 9: X-ray diffraction patterns obtained for the DPoPE lipid system alone and in the presence of the two peptides studied: DPoPE (A) at 18 °C, (B) at 42 °C, and (C) at 50 °C; DPoPE/SIVmutV, $R = 10^{-2}$ (D) at 18 °C, (E) at 42 °C, and (F) at 50 °C; and DPoPE/SIVwt, $R = 10^{-2}$ (G) at 18 °C, (H) at 42 °C, and (I) at 50 °C.

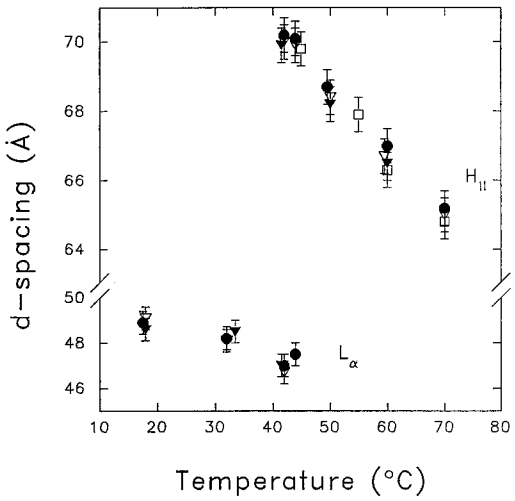

FIGURE 10: *d*-Spacing calculated from the X-ray diffractograms obtained from DPoPE alone and in the presence of the two forms of SIV fusion peptide studied, respectively: (●) DPoPE; (▽) DPoPE/SIVmutV, $R = 10^{-2}$; (▼) DPoPE/SIVwt, $R = 10^{-2}$; and (□) DPoPE/SIVwt, $R = 5 \times 10^{-2}$. The *d*-spacings were calculated using the Bragg law: $2d \sin \theta = n\lambda$.

angle reflections are very poorly resolved, but we speculate that they belong to a cubic lattice, comparable to that observed for MeDOPE. The lowest angle reflection observed corresponds to a *d*-spacing of ∼120 Å. At the phase transition temperature, the system is more ordered, and above T_H the systems transits to the hexagonal phase. The observation of an "ordered" phase transition is consistent with the fact that a cubic phase is present at lower temperatures. It is interesting to note that the DPoPE system has not been as thoroughly studied as the MeDOPE, and, to our knowledge, the observation of cubic phase formation for this lipid has not been reported thus far. Nevertheless, it

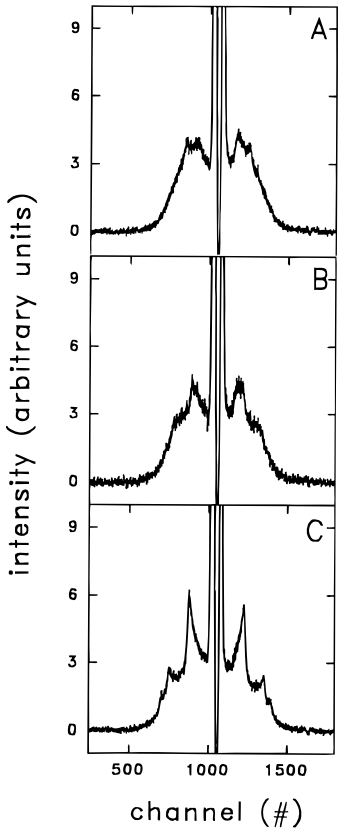

FIGURE 11: X-ray diffraction profiles obtained from the system DPoPE/SIVwt, $R = 5 \times 10^{-2}$ at different temperatures: (A) 30 °C; (B) 45 °C; and (C) 70 °C.

has been suggested that cubic phases can be induced in any lipid system presenting an $L_\alpha - H_{II}$ phase transition, by submitting the specimen to specific thermal treatments (Shyamsunder et al., 1988).

CONCLUSION

The effect of the SIVwt and SIVmutV peptides on the polymorphic behavior of different lipid systems has been studied. Our results show that both peptides have a bilayer destabilizing effect. However, while the wild-type peptide destabilizes the bilayer by inducing a negative curvature in the affected monolayer, the SIVmutV, destabilizes the bilayer by inducing a positive curvature. The bilayer destabilizing effect of the wild-type peptide has been explained in terms of its mode of insertion into the membrane, which is oblique to the normal of the bilayer (Martin et al., 1994). It has been suggested that a possible mechanism by which peptides inserted into membranes at an oblique angle may perturb bilayer structures is by expanding the center of the bilayer more than the bilayer surface, thus increasing negative curvature strain and destabilizing the bilayer relative to the formation of inverted phases. This is in agreement with our observations. The mutant-V peptide, which has been shown to penetrate the membrane with an orientation normal to the bilayer (Martin et al., 1994) also destabilizes the bilayer structure, causing it to become less ordered. However, contrary to the SIVwt, this peptide induces a positive curvature strain in the affected monolayer, thus causing a destabilization of the bilayer which does not lead to the formation of inverted phases. We suggest that a possible reason why peptides inserted into membranes along the bilayer normal disturb the bilayer structure is due to a mismatch between the length of the peptide and that of the

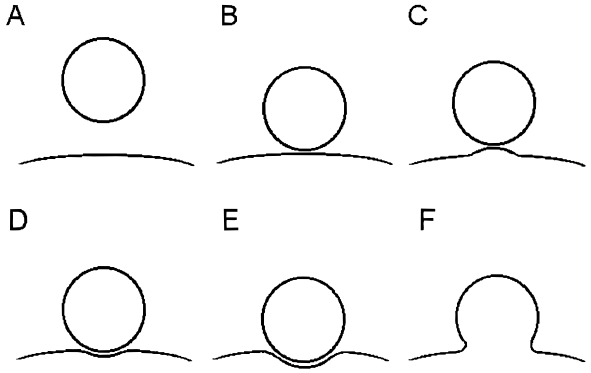

FIGURE 12: Model for the mechanism through which the membrane curvature modulatory action of fusogenic peptides and nonfusogenic peptides or fusion inhibiting compounds affect fusion. (A) Virus approaching an almost flat cell membrane surface. (B) Virus in contact with cell membrane. (C) Initial approach of virus causing positive curvature in the target membrane. This arrangement will be stabilized by SIV_{mutV} and will be destabilized by SIV_{wt} to continue along the path to final fusion, i.e., to D, E, and F. (D) An active fusion peptide induces negative curvature strain curving the cell surface towards the virion. (E) This negative curvature results in an increased area of contact between the virus and target membrane, and (F) fusion takes place.

interacting monolayer. In Figure 12 we offer a model to explain how membrane curvature modulation affects viral fusion. According to our model, peptides and other compounds which induce positive curvature strain will be good inhibitors of viral fusion, because they will locally curve the cell membrane in the direction opposite to that where the virion is approaching, preventing multiple contacts between viral proteins and the target membranes and the creation of a contact area which is large enough for fusion to occur (Figure 12C). This is in accord with the observation that a variety of amphiphiles, peptides, and proteins that raise T_H are also inhibitors of viral fusion (Epand, 1992). Fusion peptides which induce a negative curvature strain cause the membrane to curve toward the virion, allowing for a greater contact area between the two membranes (Figure 12D−E).

Another important result from this work is the dependence of the effects observed on the lipid system studied. Three lipid systems have been investigated. Although the overall conclusions for the three lipid systems converge, the peptide effect on each system was characteristic of the lipid, probably as a consequence of differences in the water/membrane interface and bending energy. Effects of the peptides are weaker for the pure PE system studied (DPoPE), where a large number of hydrogen bonds accounts for a more stable interface. The effects are stronger for the binary lipid system (DOPE/DOPC 3:1) and even more so for the MeDOPE MLVs. For MeDOPE, the peptide has easier access to the membrane/water interface, since the hydrogen bonding is weaker due to the presence of the CH_3 group on the headgroup nitrogen.

It is known that lipids are actively involved in the fusion process. It is usually proposed that transient lipid rearrangements are required for membrane fusion (Siegel, 1993). This process may be facilitated by increased negative curvature strain (Chernomordik et al., 1995). We suggest that negative curvature strain induced by viral fusion peptides may accelerate fusion even before the formation of a fusion pore. This may occur first as a consequence of fusion peptide insertion into structures such as those shown in Figure 12C. A positive curvature is formed in the target membrane upon

approach of the virus (Burger, 1996). If this occurs prior to the insertion of the fusion peptide, then the membrane with induced positive curvature will be destabilized by the spreading of headgroups in the outer monolayer. This destabilization will be accentuated by insertion of SIV_{wt} which promotes a further imbalance between the cross-sectional area in the center of the membrane and at the membrane interface. As a consequence, the membrane will be transformed from one with a positive curvature to an intermediate with a negative curvature. This will facilitate increased contact between the viral and target membrane (Figure 12D,E). Such a process was first observed by Haywood (1974) and has also been reported by us (Cheetham et al., 1994). It is likely that this morphological change is a consequence of multiple sites of attachment between the HN protein of Sendai Virus and sialic acid-containing glycolipids and glycoproteins in the target membrane. Because of the difference in size between the virus and the target cell, the presence of a high density of HN proteins in the viral envelop will cause the target membrane to envelop the virus. It is to be noted that this does not occur at coated pits and is not a precursor to endocytosis (Haywood, 1974).

In the case of influenza virus, it has been shown that several trimers of the viral fusion protein HA are required to produce membrane fusion (Ellens et al., 1990). In the case of Sendai virus, it has also been shown that there is an accumulation of the viral fusion protein at the site at which membrane fusion proceeds (Aroeti & Henis, 1991). The greater area of contact between viral and target membranes will increase the probability of having a region of the virus which is enriched in the F-protein simultaneously inserting into the target membrane. In addition, the envagination will produce a region of high curvature at which membrane fusion may commence (Haywood & Boyer, 1981). A suggested role of the fusion peptide, supported by the present study, is to facilitate the adoption of this curved structure in the target membrane. This is a consequence of increased negative curvature strain induced by the fusion peptide in the external monolayer of the cell membrane.

ACKNOWLEDGMENT

We thank Drs. Chernomordik and Haywood for providing us with preprints of their manuscripts.

REFERENCES

Anderson, D. M., Gruner, S. M., & Leibler, S. (1988) *Proc. Natl. Acad. Sci. U.S.A. 85*, 5364−5368.
Aroeti, B., & Henis, Y. I. (1991) *J. Biol. Chem. 266*, 15845−15849.
Brasseur, R., Vandenbranden, M., Cornet, B., Burny, A., & Ruysschaert, J.-M. (1990) *Biochim. Biophys. Acta 102*, 267−273.
Brown, P. M., Steers, J., Hui, S. W., Yeagle, P. L., & Silvius, J. R. (1986) *Biochemistry 25*, 4259−4267.
Burger, K. N. J. (1996) in *Lipid Polymorphism and Biological Phenomenon* (Epand, R. M., Ed.) JAI Press, Greenwich, CT.
Cheetham, J. J., Nir, S., Johnson, E., Flanagan, T. D., & Epand, R. M. (1994) *J. Biol. Chem. 268*, 5467−5472.
Chernomordik, L. V., Vogel, S. S., Leikina, E. A., Sokoloff, A., Onoran, H. O., & Zimmerberg, J. (1993) *FEBS Lett. 318*, 71−76.
Chernomordik, L., Kozlov, M. M., & Zimmerberg, J. (1995) *J. Membr. Biol. 146*, 1−14.
Düzgünes, N. (1985) in *Subcellular Biochemistry* (Roodyn, D. B., Ed.) pp 195−286, Plenum, London.
Ellens, H., Bentz, J., Mason, D., Zhang, F., & White, J. (1990) *Biochemistry 29*, 9697−9707.
Epand, R. M. (1985) *Biochemistry 24*, 7092−7095.
Epand, R. M. (1990) *Chem. Phys. Lipids 52*, 227−230.
Epand, R. M. (1992) in *Membrane Interactions of HIV: Implications for Pathogenesis and Therapy in AIDS* (Aloia, R. C., & Curtain, C. C., Eds.) pp 99−112, Wiley-Liss, New York.
Epand, R. M., & Epand, R. F. (1994) *Biochem. Biophys. Res. Commun. 202*, 1420−1425.
Epand, R. M., Cheetham, J. J., Epand, R. F., Yeagle, P. L., Richardson, C. D., Rockwell, A., & DeGrado, W. F. (1992) *Biopolymers 32*, 309−314.
Epand, R. F., Martin, I., Ruysschaert, J.-M., & Epand, R. M. (1994) *Biochem. Biophys. Res. Commun. 205*, 1938−1943.
Gagne, J., Stamatatos, L., Diacovo, T., Hui, S. W., Yeagle, P. L., & Silvius, J. R. (1985) *Biochemistry 24*, 4400−4408.
Gruener, S. M., Tate, M. W., Kirk, G. L., So, P. T. C., Turner, D. C., & Keane, D. T. (1988) *Biochemistry 27*, 2853−2866.
Gruner, S. M. (1992) in *The Structure of Biological Membranes* (Yeagle, P. L., Ed.) pp 211−250, CRC Press, Boca Raton, FL.
Guinier, A. (1963) *X-ray Diffraction in Crystals, Imperfect Crystals and Amorphous Bodies*, W. H. Freeman, San Francisco, CA.
Hartung, J., Helfrich, W., & Klösgen, B. (1994) *Biophys. Chem. 49*, 77−81.
Haywood, A. M. (1974) *J. Mol. Biol. 893*, 427−436.
Haywood, A. M., & Boyer, B. P. (1981) *Biochim. Biophys. Acta 646*, 31−35.
Hoekstra, D., & Wilschut, J. (1989) in *Water Transport in Biological Membranes* (Benga, G., Ed.) pp 143−176, CRC Press, Boca Raton, FL.
Horth, M., Lambrecht, V., Chuan Lay Khim, M., Bex, F., Thiriart, C., Ruysschaert, J.-M., Burny, A., & Brasseur, R. (1991) *EMBO J. 10*, 2747−2755.
Hui, S. W., Stewart, T. P., & Boni, L. T. (1983) *Chem. Phys. Lipids 33*, 113−126.
Hui, S. W., Isac, T. V., Boni, L. T., & Sen, A. (1985) *J. Membr. Biol. 84*, 137−146.
Marsh, M., & Helenius, A. (1989) *Adv. Virus Res. 36*, 107−151.
Martin, I., & Ruysschaert, J.-M. (1995) *Biochim. Biophys. Acta* (in press).
Martin, I., Defrise-Quertain, F., Mandieau, V., Nielsen, N. M., Saermark, T., Burn, A., Brasseur, R., Ruysschaert, J.-M., & Vandenbranden, M. (1991) *Biochem. Biophys. Res. Commun. 175*, 872−879.
Martin, I., Defrise-Quertain, F., Nielsen, N.-M., Saermark, M., Vanderbranden, M., Brasseur, R., & Ruysschaert, J.-M. (1992) *Adv. Membr. Fluid. 6*, 365−376.
Martin, I., Dubois, M.-C., Saermark, T., Epand, R. M., & Ruysschaert, J.-M. (1993) *FEBS Lett. 222*, 325−330.
Martin, I., Dubois, M. C., Defrise-Quertain, F., Saermark, T., Burny, A., Brasseur, R., & Ruysschaert, J.-M. (1994) *J. Virol. 68*, 1139−1148.
Nieva, J. L., Nir, S., Muga, A., Goñi, F. M., & Wilschut, J. (1994) *Biochemistry 33*, 3201−3209.
Ohnishi, S. (1988) in *Membrane Fusion in Fertilization, Cellular Transport and Viral Infection* (Düzgünes, N., & Bronner, F., Eds.) pp 257−296, Academic Press, New York.
Rand, R. P., Fuller, N., Parsegian, V. A., & Rau, D. C. (1988) *Biochemistry 27*, 7711−7722.
Sen, A., Hui, S. W., Mannock, D. A., Lewis, R. N. A. H., & McElhaney, R. N. (1990) *Biochemistry 29*, 7799−7804.
Shyamsunder, E., Gruner, S. M., Tate, M. W., Turner, D. C., So, P. T. C., & Tilcock, C. P. S. (1988) *Biochemistry 27*, 2332−2336.
Siegel, D. P. (1993) *Biophys. J. 65*, 2124−2140.
Siegel, D. P., & Banschbach, J. L. (1990) *Biochemistry 29*, 5975−5981.
Silvius, J. R., & Brown, P. M. (1986) *Biochemistry 25*, 4249−4258.
Tate, M. W., & Gruner, S. M. (1987) *Biochemistry 26*, 231−236.
Van Gorkom, L. C. M., Nie, S.-Q., & Epand, R. M. (1992) *Biochemistry 31*, 671−677.
Wharton, S. A., Martin, S. R., Ruyrok, R. W. H., Skehel, J. J., & Wiley, D. C. (1988) *J. Gen. Virol. 69*,1847−1857.
White, J., Kielian, M., & Helenius, A. (1983) *Q. Rev. Biophys. 16*, 151−195.
Yeagle, P. L., Smith, F. T., Young, J. E., & Flanagan, T. D. (1994) *Biochemistry 33*, 1820−1827.

BI951991+